The next generation GBCA from Guerbet is here
Explore new possibilities
© Guerbet 2024 GUOB220151-A
Guerbet

AJNR

The Perianeurysmal Environment: Influence on Saccular Aneurysm Shape and Rupture

D. San Millán Ruíz, H. Yilmaz, A.R. Dehdashti, A. Alimenti, N. de Tribolet and D.A. Rüfenacht

AJNR Am J Neuroradiol 2006, 27 (3) 504-512
http://www.ajnr.org/content/27/3/504

This information is current as of March 20, 2024.

ORIGINAL RESEARCH

D. San Millán Ruíz
H. Yilmaz
A.R. Dehdashti
A. Alimenti
N. de Tribolet
D.A. Rüfenacht

The Perianeurysmal Environment: Influence on Saccular Aneurysm Shape and Rupture

PURPOSE: The purpose of this study was to evaluate whether interactions between intracranial cerebral saccular aneurysms and the perianeurysmal environment (PAE), in the form of contact constraints, influence aneurysm shape and risk of rupture.

METHODS: A total of 190 consecutive aneurysms during a 34-month period were retrospectively analyzed. Of these, 124 were ruptured (group 1) and 66 were unruptured (group 2). Pretreatment high-resolution CT angiography was available for each aneurysm and was the determinant inclusion criterion. Aneurysm size and location, type of hemorrhage, initial Glasgow Coma Scale rating, World Federation of Neurological Societies grade, Fisher grade, and presence of concomitant aneurysms were recorded. Contact constraints between aneurysms and anatomical structures of the PAE were identified for each aneurysm and further subdivided into balanced or unbalanced depending on whether contact constraints occurred symmetrically on the aneurysm wall. Regular or irregular shape was recorded and correlated to contact constraints.

RESULTS: Compared with unruptured aneurysms, ruptured aneurysms were found to be larger and more irregular, to develop more contact constraints with the PAE, and to show higher rates of unbalanced contact constraints. Ruptured aneurysms had a tendency to be found in locations of a constraining PAE. Irregular shape was positively correlated with the presence of an unbalanced contact constraint, even in the absence of obvious contour deformations from an imprint of an adjacent structure.

CONCLUSION: The existence of contact constraints between intracranial saccular aneurysms and the PAE were shown to influence shape and risk of aneurysm rupture. Modifications of wall shear stress by contact constraints are discussed. Analysis of contact constraints between aneurysm and the PAE could be considered additional parameters in the assessment of risk of aneurysm rupture.

The prevalence of unruptured intracranial aneurysms in the general population, as reported by a recent review,[1] ranges between 3% and 6.6%, which represents 3000 to 6600 cases when extrapolated to a population of 100,000 persons. The incidence of ruptured aneurysms is, however, low, with approximately 10 cases in every 100,000 persons per year,[1,2] which suggests that very few aneurysms rupture. Unruptured intracranial aneurysms may be diagnosed clinically in a setting of subarachnoid hemorrhage (SAH) caused by the rupture of another existing aneurysm, during screening in a setting of positive family history of ruptured intracranial aneurysm or autosomal dominant polycystic kidney disease, in the investigation of clinical symptoms relative to cranial nerve compression or hydrocephalus related to the aneurysm, or may be diagnosed fortuitously during routine CT or MR imaging investigations for problems unrelated to the aneurysm. Whatever the case, unruptured intracranial aneurysms represent a dilemma for the physicians, who have to weigh the risk of aneurysm rupture with respect to its natural history against the risk of morbidity and mortality from an endovascular or surgical repair.

With CT and MR imaging being more frequently and widely used, a growing number of intracranial aneurysms are being diagnosed, posing the problem of which aneurysms harbor a sufficiently high risk of rupture to merit endovascular or surgical repair. Recent publications have addressed this issue and have demonstrated that, among other variables affecting the natural history of aneurysms, aneurysm size and location represent independent predictors of both risk of rupture and surgical/endovascular repair outcomes.[3,4] Other parameters, such as irregular aneurysm shape and, in particular, the presence of blebs, are recognized as translating an area of weak wall structure and high risk of rupture.[5]

A parameter that has not yet been clearly assessed in the literature is how aneurysms interact with their environment and whether such interactions could influence their natural history. Intracranial saccular aneurysms develop in the subarachnoid space, which is divided into subarachnoid cisterns that are bounded by arachnoid, bone, brain, and dura and are traversed by arachnoid villi, cranial nerves, and vessels. The subarachnoid space forms the medium or the perianeurysmal environment (PAE) in which aneurysms grow and eventually rupture. It would be logical for the PAE to vary for each aneurysm location. As an aneurysm grows, it may encounter one or more anatomic structures of the PAE. For instance, a cranially oriented giant basilar tip aneurysm (BTA) would be expected to grow between the cerebral peduncles and embed into the floor of the third ventricle; similarly, a caudally oriented anterior communicating artery (AcomA) aneurysm may encounter the optic chiasma or the planum sphenoidale in its course.

Symptoms resulting from the interaction of unruptured intracranial aneurysm with the PAE are well known clinically. Bony erosions in the vicinity of an aneurysm, cranial nerve compression, or obstructive hydrocephalus caused by large

Received March 14, 2005; accepted after revision August 14.

From the Section of Neuroradiology, Department of Radiology and Medical Informatics (D.S.M.R., H.Y., A.A., D.A.R.), and the Department of Neurosurgery (N.d.T.), Geneva University Hospital, Geneva, Switzerland; and the Department of Neurosurgery, Lausannne University Hospital (A.R.D.), Lausanne, Switzerland.

Financial support was granted by William COOK Europe A/S, Bjaeverskov, Denmark.

Address correspondence to Diego San Millán Ruíz, MD, Section of Neuroradiology, Department of Radiology and Medical Informatics, Geneva University Hospital, 24, rue Micheli-du-Crest, 1211 Geneva 14, Switzerland.

aneurysms are well documented in the literature[6,7] and are demonstrative of the pressure ensuing from the contact constraints that develop between the aneurysm and the adjacent structures. Remarkably little is mentioned on how the natural history of an aneurysm may be altered by contact constraints developing between an aneurysm and the PAE. Such contact constraints may be expected to modify the shape of an aneurysm and influence the biomechanical stability of the aneurysm wall. Alterations of the stress distribution throughout the aneurysm wall could provide either a protective effect or, inversely, a detrimental effect. Seshaiyer and Humphrey,[8] by using finite element analyses of stress fields in a mathematical model, have shown how certain contact constraints, when applied to an axisymmetric aneurysm at the level of the fundus, may decrease stresses and provide a protective effect.[8] Inversely, a contact constraint uniformly distributed could increase focal stresses around the aneurysm wall and lead to aneurysm rupture.

Several clinical observations suggest that the PAE may affect the natural history of intracranial aneurysms. For instance, perioperative aneurysm rupture is well known to neurosurgeons at the moment that they mobilize adjacent brain parenchyma to access the aneurysm neck for clipping. In such instances, the contact between the aneurysm with the adjacent brain parenchyma is abruptly modified, with, possibly, a subsequent alteration of existing contact constraints and wall stress distribution, followed by aneurysm rupture. A similar mechanism may be observed during a Valsalva maneuver that is clinically followed by an aneurysm rupture. Again, the abrupt modification of the PAE after the concomitant increase of brain blood volume with a proportional reduction in the volume of the subarachnoid spaces during the Valsalva maneuver may alter the equilibrium of the various forces acting around the aneurysm wall and bring about a tear. Finally, there is a gradual decrease in the risk of aneurysm rupture during the eighth and ninth decades, possibly because, with age-related brain atrophy, there is an increase in volume of the subarachnoid space, and thus unfavorable contact constraints between an aneurysm and its PAE are less likely to occur.

The purpose of this article is to identify whether contact constraints, developing between intracranial saccular aneurysms and the PAE, influence aneurysm shape and risk of rupture.

Materials and Methods

Patients and Technique

All patients who underwent high-resolution, multisection CT angiography (HRCTA; Philips, Best, the Netherlands) in our institution between January 2003 and November 2005 and who harbored an intracranial saccular aneurysm were included in this retrospective analysis. Brain CT leading to the suspected or fortuitous diagnosis of intracranial aneurysms was performed for the following reasons: suspected SAH; symptoms due to mass effect related to the aneurysm; headache of unknown etiology and not related to SAH; search for metastasis, cerebral ischemia unrelated to the aneurysm, or adult dominant polycystic kidney disease. An aneurysm diagnosed during the specified period was included if high-quality pretreatment HRCTA was available. Excluded from this study were all fusiform, posttraumatic, and mycotic aneurysms, as well as caroticocavernous aneurysms.

The protocol consisted of noncontrast 3-mm-thick sections, followed by injected HRCTA acquisition by using bolus tracking (140 mL of contrast product at 5 mL/s) and 1.5-mm-thick sections every 0.75 mm, starting at the carotid bifurcation and going up to the vertex. Finally, 5-mm-thick sections were obtained 120 seconds after beginning the contrast product injection.

Analysis of the radiologic data were performed by 2 trained radiologists (D.S.M.R. and H.Y.). All data were analyzed electronically on a PACS station (Cedara, Ontario, Canada) allowing for axial plane image visualization and 3-plane multiplanar reconstructions (MPRs). 3D reconstructions were also obtained after transfer to a Vitrea workstation (Vital Images, Minnetonka, Minn). Type of hemorrhage, initial Glasgow Coma Scale (GCS) rating, World Federation of Neurological Societies (WFNS) grade, Fisher grade, and presence of concomitant aneurysms were recorded.

Aneurysms were separated into 2 groups, ruptured versus unruptured, based on confirmation of a SAH at presentation. When more than one aneurysm was found in the presence of SAH, the following criteria were used to identify the aneurysm that had ruptured: the aneurysm found in the region where there was the largest volume of subarachnoid blood; presence of bleb or irregular shape; the most proximally located aneurysm; demonstration of extravasation of contrast product translating active bleeding.

Aneurysm location, size, shape, and contact with the PAE were analyzed for ruptured and unruptured aneurysm. Aneurysm dome size was measured in the 3 axes, and maximum dome size was determined by the longest diameter. Aneurysm neck dimension was recorded. Shape was classified either as regular or irregular. Irregular aneurysms were defined as aneurysms with multiple irregularities due to several bleb formations, impressions from contact with elements of the PAE, or a combination of both. Particular attention was given to aneurysm contour deformation by incompressible anatomical structures of the PAE, such as bone or dura. The inverse (ie, PAE deformation by an aneurysm, particularly bony erosions) was also identified.

Interaction between aneurysms and the PAE was established by the presence or absence of contact constraints between the aneurysmal wall and the surrounding anatomic structures such as bone, dura mater, brain, vessels, or nerves. Contact constraints were identified when the shape of an aneurysm was modified by the imprint of an adjacent structure, when an aneurysm eroded adjacent bone, or when an aneurysm was found to abut an adjacent structure of the PAE. Contact was qualified as balanced or unbalanced. Balanced and unbalanced contact constraints were determined depending on whether a contact occurred symmetrically on the aneurysm wall: for instance, a contact constraint applied on the lateral wall of the aneurysm was considered unbalanced, whereas a contact constraint applied to the fundus or applied circumferentially was considered balanced because it did not modify the axisymmetry of the aneurysm. When several contacts were identified, if different anatomic structures were involved—brain and bone for instance—the contact constraint was considered to be unbalanced.

If a clear definition of the contact was not possible on the basis of the available imaging studies, contact was referred to as unclear. Presence of a contact constraint was correlated to aneurysm shape in an effort to determine whether aneurysm shape was influenced by contact constraints with the PAE.

Statistical Analysis

The 2 groups of aneurysms were tested for a normal distribution by using the mean maximum diameters for both groups, which were

Table 1: Distribution of aneurysm locations

Site	Group 1 (%)	Group 2 (%)
ACA	3	1.5
AchoA	<1	4.5
AcomA	**37**	**15**
AICA	2	0
PCA	2.5	3
BA tip	4	7.5
ICA	5.5	**14**
MCA	**22**	**44**
PcomA	**20**	9
PICA	3	1.5

Note:—ACA indicates anterior cerebral artery (all segments included); AchoA, anterior choroidal artery; AcomA, anterior communicating artery; AICA, anterior inferior cerebellar artery; PCA, posterior cerebral artery (all segments included); BA, basilar artery; ICA, internal carotid artery (supraclinoid portion only; PcomA and AchoA aneurysms are considered separately); MCA, middle cerebral artery (all segments included); PcomA, posterior communicating artery-ICA junction; PICA, posterior inferior cerebellar artery. Boldface type within each group indicates the first 3 more frequent locations.

plotted in a histogram. The histogram revealed a non-Gaussian distribution. Nonparametric Wilcoxon tests were therefore used for the statistical analysis.

Results

Patient Population

In the present study, 190 aneurysms from 174 patients were included, of which 124 had ruptured on presentation and 66 were found to be unruptured. Aneurysms were classified into 2 groups, one containing ruptured aneurysms (group 1) and another containing unruptured aneurysms (group 2). There were 124 patients in group 1 and 50 in group 2. Thirty-one of the 50 patients (62%) harboring an unruptured aneurysm (group 2) had presented with SAH from a ruptured aneurysm at another site. The motivation behind the radiologic work-up leading to the discovery of an unruptured aneurysm in the 19 remaining patients of group 2—that is, those who did not present with SAH from a ruptured aneurysm at another site varied from mass effect caused by the aneurysm, headache of unknown etiology and not related to SAH, search for metastasis, cerebral ischemia unrelated to the aneurysm, and adult dominant polycystic kidney disease.

These 2 groups were comparable in terms of age and sex distributions. In both groups, most patients were women—65% and 69%, respectively, for groups 1 and 2—and average age was found to be 50 and 52 years, respectively, for groups 1 and 2, with an identical SD of ±13.

The initial clinical evaluation of patients in group 1 presenting with hemorrhage revealed an average WFNS grade of 1.9 (SD ± 1.3). Initial average Fisher grade on HRCT was found to be 3.1 (SD ± 1.0).

Aneurysm Location and Sizes

Aneurysm sites were found to be different for both groups. The most frequent site for ruptured aneurysms was on the AcomA (37%), followed by middle cerebral artery aneurysms (MCA) (22%) and by posterior communicating artery (PcomA) aneurysms (20%). Unruptured aneurysms were most frequently found on the MCA (44%), followed by AcomA (15%), distal ICA (14%), and PcomA (9%). Table 1 shows the distribution of the sites of ruptured and unruptured aneurysms.

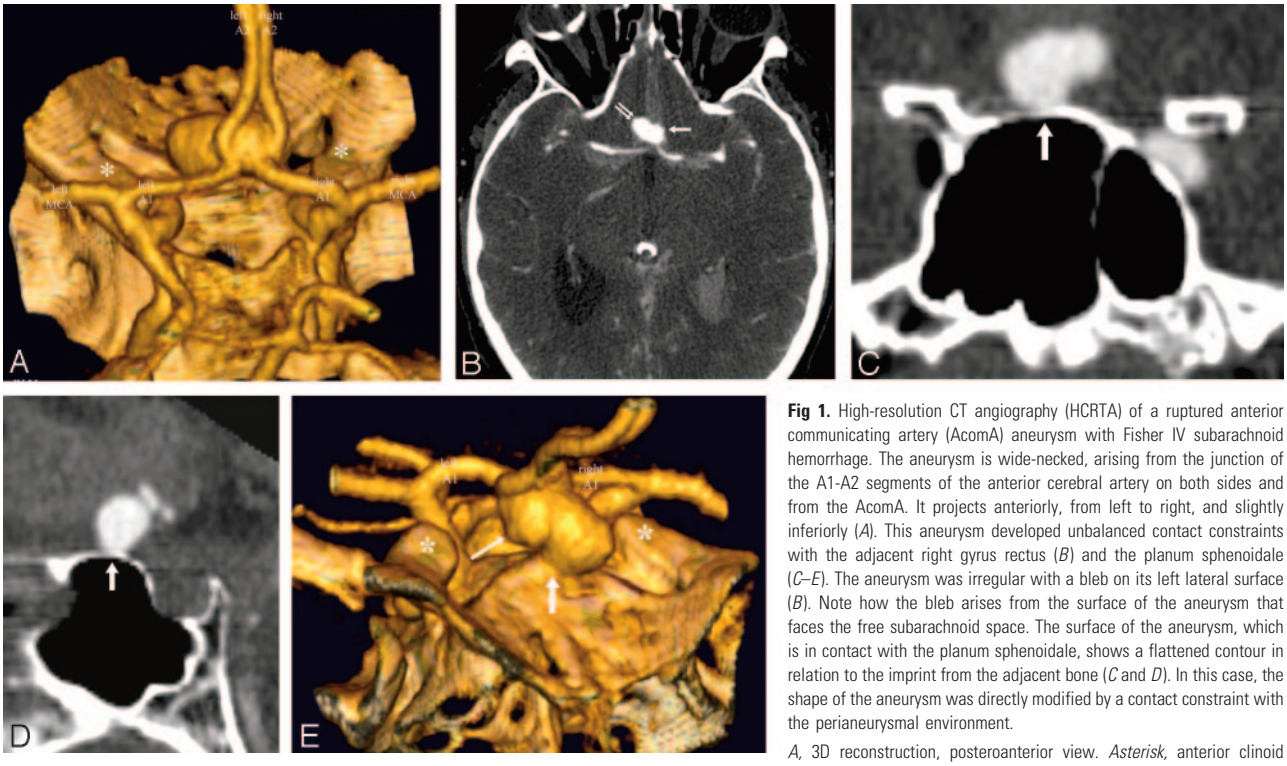

Fig 1. High-resolution CT angiography (HCRTA) of a ruptured anterior communicating artery (AcomA) aneurysm with Fisher IV subarachnoid hemorrhage. The aneurysm is wide-necked, arising from the junction of the A1-A2 segments of the anterior cerebral artery on both sides and from the AcomA. It projects anteriorly, from left to right, and slightly inferiorly (*A*). This aneurysm developed unbalanced contact constraints with the adjacent right gyrus rectus (*B*) and the planum sphenoidale (*C–E*). The aneurysm was irregular with a bleb on its left lateral surface (*B*). Note how the bleb arises from the surface of the aneurysm that faces the free subarachnoid space. The surface of the aneurysm, which is in contact with the planum sphenoidale, shows a flattened contour in relation to the imprint from the adjacent bone (*C* and *D*). In this case, the shape of the aneurysm was directly modified by a contact constraint with the perianeurysmal environment.

A, 3D reconstruction, posteroanterior view. *Asterisk,* anterior clinoid processes.

B, Axial HCRTA. *Single arrow,* bleb; *double arrow,* unbalanced contact constraint with gyrus rectus.

C and *D,* Coronal and sagittal plane multiplanar reconstructions. *White arrow,* contour deformation of the surface of the aneurysm in contact with the planum sphenoidale.

E, 3D reconstruction, anteroposterior, slightly oblique view. *Small arrow,* bleb; *large arrow,* contact constraint with planum sphenoidale.

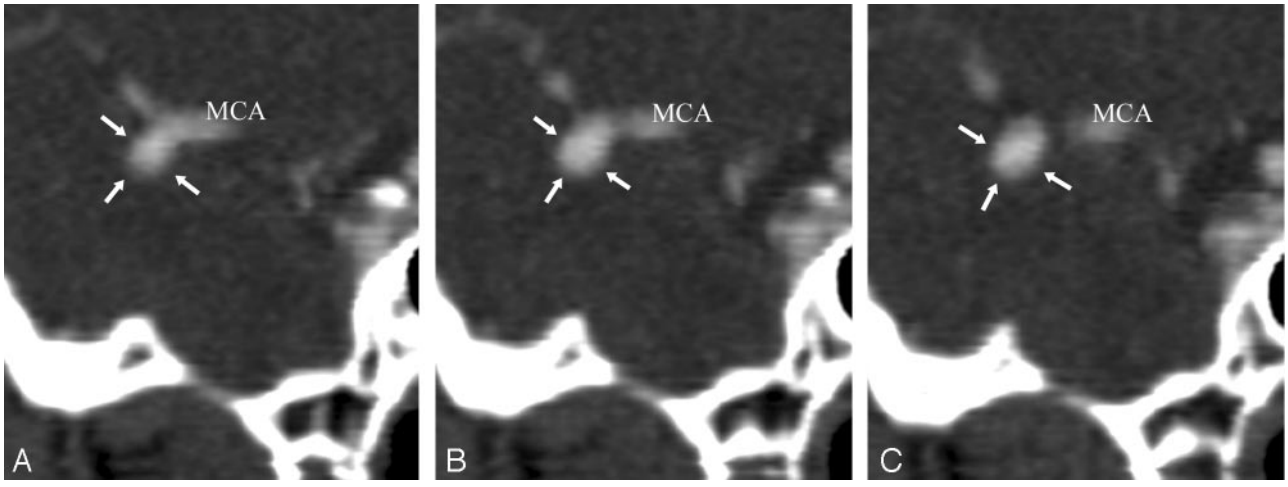

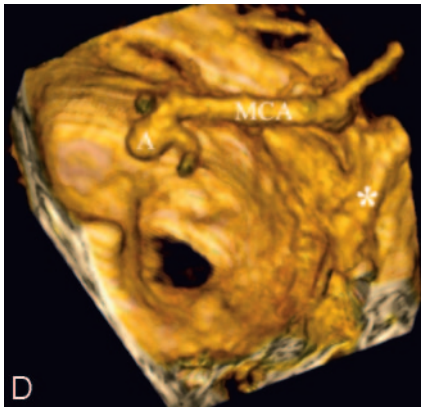

Fig 2. A 47-year-old man with chronic headache. A left, unruptured middle cerebral artery (MCA) aneurysm was suspected during routine CT, which motivated high-resolution CT angiography (HCRTA). HRCTA revealed a 6-mm MCA aneurysm, which pointed inferiorly and was embedded in the temporal lobe (*A–D*). The whole circumference of the aneurysm was surrounded by brain tissue, resulting in a balanced contact constraint (*A–C*). This aneurysm had regular contours.

A–C, Sequential, coronal plane, multiplanar reconstructions of HRCTA. *arrows,* balanced contact constraint with surrounding temporal lobe parenchyma.

D, Three-dimensional reconstruction of HRCTA, left superior view. *A,* MCA aneurysm; *asterisk,* posterior clinoid process.

Ruptured aneurysms were an average of 1.4 mm larger than unruptured aneurysms, with an average maximum aneurysm diameter of 7.6 mm (SD ± 4.1) versus 6.1 mm (SD ± 5.5). The difference in size was statistically significant ($P < .002$, with a confidence interval of 95%). Average neck dimensions were similar in both groups, measuring 3.1 mm (SD ±1.1) for the ruptured aneurysms against 3.2 mm (SD ± 1.6).

Contact with the PAE, Balanced and Unbalanced Contact

Contact between aneurysm and elements in the PAE occurred in 87% of group 1 aneurysms (109 of 124 aneurysms) compared with 68% of group 2 (45 of 66 aneurysms). The greatest difference between the 2 groups was found in the types of contact constraints that developed between aneurysms and the PAE. Contacts in group 1 aneurysms were found to be unbalanced 91% of the time versus 38% in group 2 (Figs 1–3). In group 1, contact type could not be determined in 3% of the cases, because of the limitations of HRCT to clearly delineate surrounding anatomic structures or because of the presence of a large blood clot around the aneurysm. Contact constraints with adjacent nerves were hardest to determine. Nerves could clearly be identified when the surrounding blood clot delineated them as a "negative print" (Fig 4). On rare occasions, nerves could be demonstrated by using coronal plane MPRs of HRCTA images (Fig 5). Whenever this was impossible, the trajectory of the nerve was traced relative to surrounding anatomic landmarks, and a contact constraint was retained if an aneurysm bisected this virtual line.

In group 1, ruptured aneurysms without contact were found to have smaller average maximum dome sizes than the average maximum dome size for the entire group, at 4.3 mm versus 7.6 mm. Aneurysm sites were found to be the following: AcomA, 46.7%; ICA bifurcation, 20.0%; MCA bifurcation, 13.3%; PICA, 6.6%; basilar tip, 6.6%; and PCA, 6.6%. Group 2 aneurysms without contact were also significantly smaller than aneurysms of the same group, with an average maximum dome size of 3.3 mm versus 6.1 mm.

Aneurysm Shape and Shape in Relation to Contacts with the PAE

Most group 1 aneurysms were found to have an irregular shape (71.8% of the time; 0–4 blebs), and most group 2 aneurysms were found to be regularly shaped (72.7% of the time; 1–3 blebs). Blebs typically developed in areas devoid of any contact with the PAE—that is, facing the subarachnoid space. Aneurysm contour deformation and PAE deformation developing from contact constraints between aneurysms and the PAE are summarized in Table 2 (Fig 6).

In both groups, irregular shape was more frequently found in aneurysms that developed contacts with the PAE, with 92% and 94.4% in groups 1 and 2, respectively. Inversely, regular-shaped aneurysms were encountered less frequently in the presence of contact with the PAE, 77.1% and 56.2% in groups 1 and 2, respectively. In group 1, irregular shape was also correlated with unbalanced contact, and 83.1% of irregular shaped aneurysms demonstrated an unbalanced contact. In group 2, numbers of irregular shaped aneurysms were insufficient to draw any statistically significant conclusions.

Discussion

The present study was aimed at demonstrating that intracranial saccular aneurysms interact with the PAE by developing contact constraints with surrounding anatomic structures, which may modify the natural history of an aneurysm. A population of 124 ruptured intracranial saccular

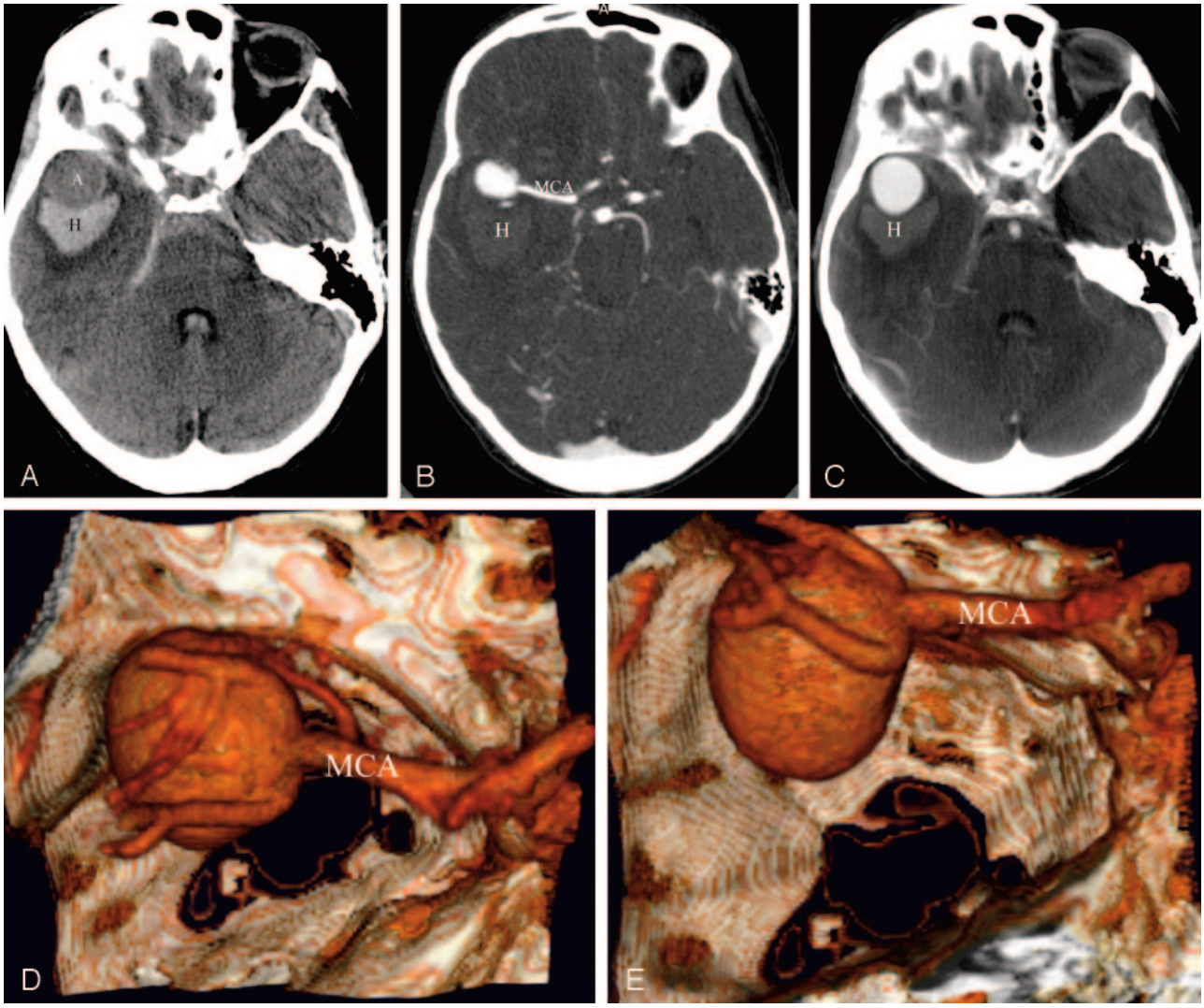

Fig 3. Ruptured, right-sided giant middle cerebral artery (MCA) bifurcation aneurysm with right, intraparenchymal temporal lobe hematoma. On noncontrast CT, the aneurysm was seen as a round structure that was hypoattenuated compared with the temporal lobe hematoma (*A*). Postcontrast high-resolution CT angiography (HCRTA) showed an unbalanced contact constraint with the frontal and temporal lobes (*B*) and with the greater sphenoid wing (*C–E*). The aneurysm had a regular shape with no blebs. This case showed how the trajectory and growth of the aneurysm could have been influenced by the contact constraints it developed with the perianeurysmal environment. As it grew, this aneurysm was probably canalized laterally and outward by the adjacent frontal and temporal lobes that delimitate the sylvian fissure, and then, when it developed a contact constraint with the sphenoid greater wing, it grew caudally toward the middle cranial fossa.

A, Axial, noncontrast enhanced, HRCT. *A,* aneurysm; *H,* hemorrhage.

B and *C,* Axial, postcontrast HRCTA. *H,* hemorrhage.

D, 3D reconstruction of HRCTA, superior view.

E, 3D reconstruction of HRCTA, posteroanterior view.

aneurysms was studied and compared with a population of 66 unruptured aneurysms. Fusiform, posttraumatic, mycotic, and carotidocavernous aneurysms were excluded from this study. HRCTA was used in all cases to evaluate contact constraints between aneurysms and the PAE. Age and sex distributions were comparable in both groups, with a female predominance (65% and 69% of women for ruptured and unruptured aneurysms, respectively) and average age on diagnosis of approximately 50 years. Aneurysm locations were different in both groups and are summarized in Table 1; the 3 most frequent sites for ruptured aneurysms (group 1) in decreasing order of frequency were AcomA, MCA, and PcomA, whereas unruptured aneurysms (group 2) were more frequently found at a MCA, AcomA, or distal ICA location.

Contact between aneurysms and the PAE was evaluated by using HRCTA. A contact constraint was proved when aneurysmal contours were deformed by the PAE or when an aneurysm caused bony erosions. This situation, however, was not frequently observed. In aneurysms that did not present contour deformations or that did not erode bony structures, contact constraints were considered to exist whenever the aneurysm abutted an anatomic structure of the PAE, such as bone, dura mater, brain, nerve, or vessel. This was straightforward whenever the aneurysm had a contact with bone, dura mater, brain, or a vessel, which were clearly delineated. Contact constraints with a nerve was more difficult to establish. In some cases, the SAH delineated the nerve, which appeared as a "negative print" within the blood clot (Fig 4). In other cases, coronal MPRs demonstrated the nerves better than on axial images

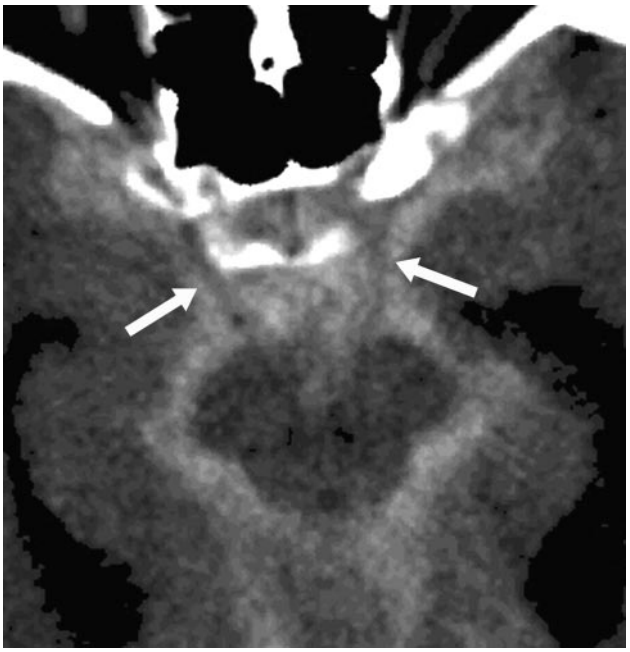

Fig 4. Axial noncontrast CT. Ruptured anterior communicating artery (AcomA) aneurysm with Fisher IV subarachnoid hemorrhage (SAH). The SAH delineates the cisternal portion of both occulomotor nerves (*white arrows*), which appear as a "negative print" within the blood clot. In such cases, contact constraints between an aneurysm with the occulomotor nerve could readily be identified.

(Fig 5). On many occasions, however, this was not the case, and the location of the nerve was estimated with respect to visible landmarks that could be used to trace the trajectory of a nerve—for instance, the interpeduncular fossa, the free edge of the tentorium, and the posterior clinoid processes in the case of the occulomotor nerve. If the aneurysm bisected the assumed location of the nerve, an existing contact constraint was retained. The difficulty in establishing the presence of a contact between an aneurysm and the PAE by using HRCTA may be one of the drawbacks of this study. High-resolution MR imaging with 3-dimensional T2-weighted images could overcome this difficulty, but access to MR imaging for all aneurysms was difficult to obtain in an emergency setting.

Whenever a contact was identified, we strove to establish whether the resulting contact constraint could have a protective or a detrimental effect on the aneurysm. In the first situation, a contact constraint acting as a reactive force counteracting aneurysmal distension pressure could be protective. Inversely, contact constraints could alter the stress distribution throughout the aneurysm wall and disrupt the equilibrium between wall strength and wall stress, leading to aneurysm rupture. The first type of "protective" contact constraint was classified as balanced and the second "detrimental" type of contact constraint as unbalanced. Balanced and unbalanced contact constraints were considered depending on whether a contact was thought to modify wall stress in such a way that stress became inharmoniously distributed throughout the aneurysm wall: for instance, a contact constraint applied on the lateral wall of the aneurysm was considered unbalanced, but a contact constraint applied to the fundus or applied circumferentially was considered balanced. When several contacts were identified, if different anatomic structures were involved, brain and bone for instance, the contact constraint was considered to be unbalanced.

Contact with the PAE was significantly more frequent in group 1 aneurysms than in group 2 aneurysms (87% vs 68%). The most striking difference between both groups was in the type of contact constraint, with group 1 aneurysms showing an unbalanced type in 91% of the cases against 38% of the cases in group 2. Thus, ruptured aneurysms showed, on the one hand, a greater proportion of contact constraints with the PAE than unruptured aneurysms and, on the other, a significantly higher rate of unbalanced type of contact constraints. There are several possible explanations for this observation. First, group 1 aneurysms were larger than aneurysms in group 2. Thus, they had a greater probability of developing a contact with the PAE. Then, ruptured aneurysms were more frequently observed in sites where the subarachnoid space is relatively tight and particularly rich in anatomic structures, a favorable PAE for the development of contacts and unbalanced contact constraints. This is well illustrated with PcomA aneurysms, which were more frequently found in group 1 than in group 2 (20.1% vs 9%). This location is particularly constraining for an aneurysm, especially if it develops posteriorly and inferiorly to the posterior wall of the ICA. Such an orientation exposes the aneurysm to bone, brain, vessels, dura mater, and nerve as it grows—that is, the free edge of the tentorium and the mediotemporal lobe laterally and inferiorly, the occulomotor nerve, and the ICA inferiorly, and the posterior clinoid process medially and inferiorly.

Balanced contact constraints were for the most part observed in unruptured aneurysms. Sixty-eight percent of group 2 aneurysms had contact with the PAE, of which 62% developed balanced contact constraints. Balanced contact constraints were therefore much more frequently observed in unruptured aneurysms than in ruptured aneurysms. MCA bifurcations were, by and large, the most frequent site of unruptured aneurysms, occurring in 44% of group 2 aneurysms. Contact constraints were balanced in 79% of MCA aneurysms, usually because contact, most often with adjacent frontal and temporal lobes, occurred around the fundus and even around the whole circumference of the aneurysm, serving as a "natural wrapping" around the aneurysm. In some of these cases, the contact constraints may have been protective against rupture by acting as a counteracting force to aneurysmal distension pressures (Fig 2). Aneurysm rupture also occurred in cases of balanced contact constraint, albeit in a small number of cases (6%).

Finally, 13% of ruptured aneurysms did not develop contacts with the PAE. Their average maximum dome size of 4.3 mm was significantly smaller than the average maximum dome size of group 1, which measured 7.6 mm. These aneurysms were too small to develop contact constraints with the PAE. This subgroup probably corresponds to aneurysms that ruptured during the initiation phase or early in the growth phase of the aneurysm, before the remodeling process of the aneurysm wall could be initiated. Several authors have demonstrated that small aneurysms with sizes similar to this subgroup have very thin walls composed mainly of endothelium and a thin adventitia,[9–11] which supports the present hypothesis.

Aneurysm wall quality was indirectly evaluated by studying

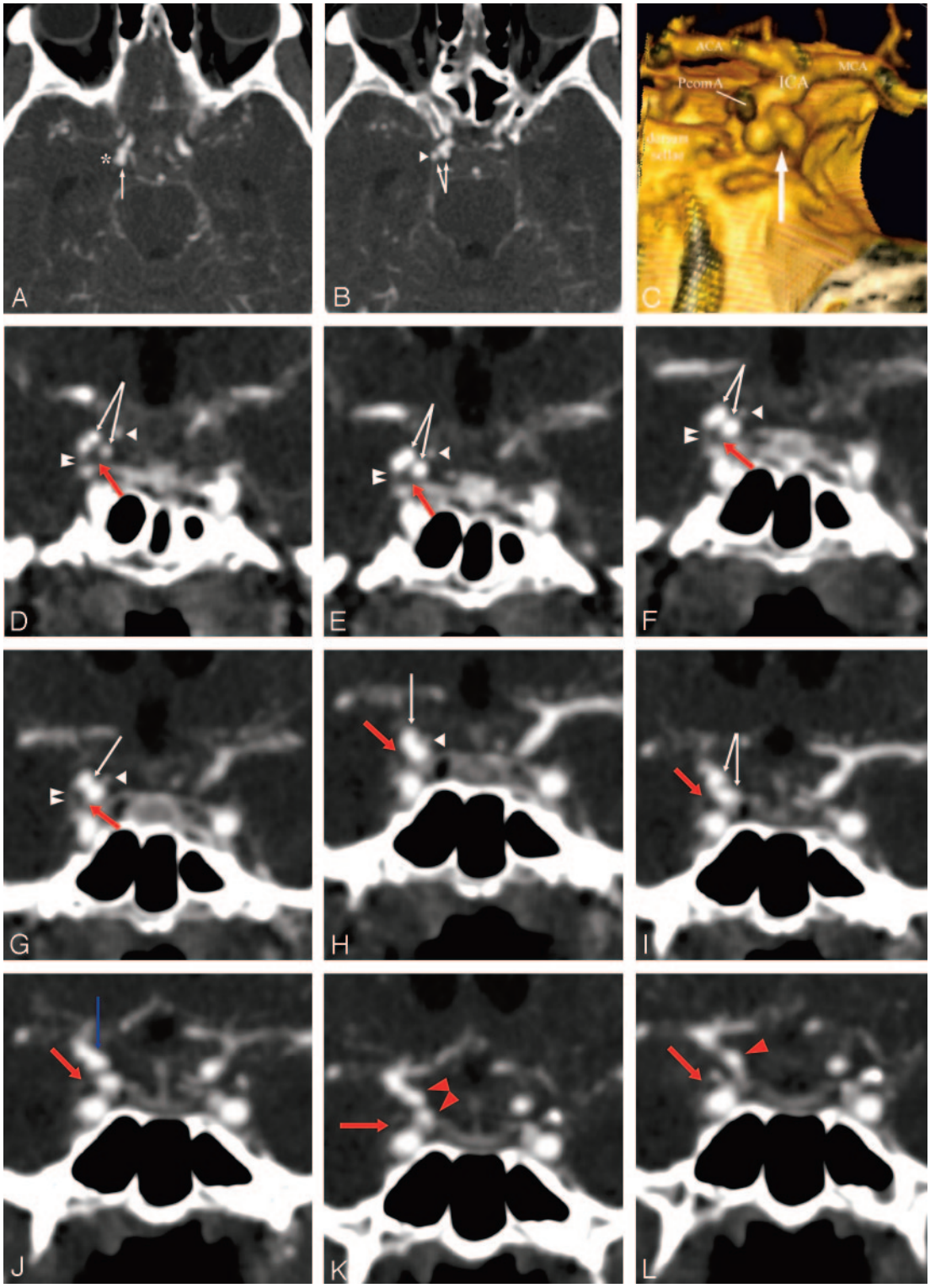

Fig 5. High-resolution CT angiography (HCRTA) of a ruptured right posterior communicating artery (PcomA) aneurysm with Fisher IV SAH. This aneurysm is highly irregular with multiple blebs (*A–C*). Axial HRCTA images show unbalanced contact constraints with the mediotemporal lobe (*A*) and the free border of the tentorium cerebelli (*B*). Coronal plane reconstructions show the occulomotor nerve as a round nonenhancing structure and the free edge of the tentorium as an enhancing, linear, slitlike structure (*D–L*). The contours of the aneurysms are clearly deformed by the imprint of these 2 structures on its inferior surface. The PcomA is visualized medially to the aneurysm.

A and *B,* Axial HRCTA images. *White arrow,* PcomA aneurysm; *asterisk,* contact with the mesiotemporal lobe; *arrowhead,* contact with the free border of the tentorium cerebelli.

C, 3D reconstruction of HRCTA, posteroanterior view. *Arrow,* imprint from free border of tentorium cerebelli and right occulomotor nerve.

D–L, Coronal plane, sequential, back to front, thin section multiplanar reconstruction of the PcomA aneurysm. *Double arrowhead,* free border of the tentorium cerebelli; *white arrowhead,* PcomA; *red arrow,* right occulomotor nerve; *white arrow,* PcomA aneurysm; red arrowhead, cisternal internal carotid artery (ICA); *blue arrow,* ICA-PcomA aneurysm junction.

Table 2: Aneurysm and PAE contour deformations

	Group 1	Group 2
No. of aneurysms with contact with bone or dura	32	4
Contour deformation of the aneurysm	20 (62.5%)	2 (50%)
Deformation of the PAE by aneurysm (bone erosion)	5 (15.6%)	2 (50%)
Location		
PcomA	9 (45%)	—
AcomA	5 (25%)	—
ICA/ophthalmic	1 (5%)	2 (100%)
ICA C1/C2	1 (5%)	—
MCA	3 (15%)	—
PCA P1/P2	1 (5%)	—

Note:—PAE indicates perianeurysmal environment; PcomA, posterior communicating artery; AcomA, anterior communicating artery; ICA, internal carotid artery; MCA, middle cerebral artery; PCA, posterior cerebral artery.

aneurysm shape, irregular shape being considered indicative of areas of weak wall structure and points of high shear stress.[12] Irregular shape was found to be highest in ruptured aneurysms (75% of the aneurysms), whereas only a minority of unruptured aneurysms were irregularly shaped (27% of the aneurysms). Group 1 aneurysms were larger than group 2 aneurysms, which is consistent with previous reports in which irregular shape was found to be significantly more frequent in larger aneurysms.[13]

Conclusions as to the influence of the PAE on the shape of the aneurysm could clearly be drawn when the contours of an aneurysm were deformed by an adjacent structure or when bony erosions adjacent to the aneurysm were noted (Figs 1, 5, and 6). Contour deformations were confirmed only in cases where the contact constraints were established with either bone or dura mater. Contact constraints with bone or dura mater were observed in 36% of group 1 irregular aneurysms and 22% of group 2 irregular aneurysms and accounted for irregular shape in 62.5% and 50%, respectively, for group 1 and 2 in this subset of aneurysms. In most irregular aneurysms, however, irregular shape was observed in the form of blebs that were not directly induced from the imprint of an adjacent structure of the PAE. In this subset of aneurysms, the influence of contact constraints on the shape of the aneurysm is more difficult to establish. Notwithstanding, both contact constraints and a high rate of unbalanced type of contact constraints were, for the most part, more frequent in irregularly shaped aneurysms than in regularly shaped aneurysms in both groups. This suggests that both the existence and the type of contact constraint influence the shape of an aneurysm.

The natural history of intracranial aneurysms involves aneurysm formation, growth, and sometimes rupture. The results of the present study suggest that the PAE may play an important role in the growth and rupture of intracranial aneurysms that are large enough to develop contact constraints with the PAE. This influence probably involves modifications of aneurysmal wall shear stress that have been demonstrated to play an important role in the genesis, growth, and rupture of intracranial aneurysms.[14–16] Wall shear stress is influenced by the shape and axisymmetry of an aneurysm, among other parameters.[17,18] Thus, when an aneurysm becomes irregular in shape because of contact constraints with the PAE, it is possible that the distribution of wall shear stress around the aneurysm wall becomes heterogeneous and favors zones of focal increased wall stress at a higher risk of rupture. Even in cases in which structures adjacent to an aneurysm do not imprint on the aneurysm wall, unbalanced contact constraints between the aneurysm and the PAE are probably sufficient to modify wall shear stress, probably through alterations in aneurysm wall pulsatility. Finally, aside from the mechanical influence of the PAE, modifications of wall shear stress could also bring about biologic changes and induce aneurysm wall remodeling. Montorzi et al[19] mention the structural asymmetry in porcine common carotid arteries in response to asymmetric conditions of shear stress related to asymmetric tissue support. The posterior wall of the common carotid artery, which was in contact with the rigid cartilaginous tissue of the trachea, was thinner than the anterior wall, which was entirely surrounded by soft tissue. Furthermore, the posterior wall was richer in elastin but poorer in collagen compared with the anterior wall. Although this observation is based on normal extracranial vessels, it could well be applicable to intracranial aneurysms, with shear stress inducing structural modifications of the matrix of the aneurysm wall and local decreases in wall strengths. Biologic modifications could also occur in the arachnoid trabeculae of the subarachnoid space in response to aneurysm formation and growth. Adherences are often observed around an unruptured aneurysm during surgery and could very well represent this kind of tissue reaction. Traction forces during aneurysm pulsation resulting from these adherences could favor aneurysm rupture.

Conclusion

The natural history of intracranial aneurysms is currently thought to be governed by many different parameters and to go through 3 successive phases: aneurysm initiation or formation, growth, and, eventually, rupture. As an aneurysm grows, it may develop contact constraints with its PAE. The present study suggests that these contact constraints may have an influence in the natural history of an aneurysm, probably in the growth and rupture phases. When comparing ruptured and unruptured aneurysms, these 2 groups were clearly distinct; ruptured aneurysms were larger and were more frequently seen to develop contact constraints with their environment, and those constraints were more frequently of the unbalanced type. Aneurysm shape was also seen to be correlated both to the presence of a contact constraint and to the unbalanced type of contact constraint. Finally, the development of contact constraints with the PAE depended on the location of the aneurysm; sites where the PAE was anatomically very tight, such as PcomA, favored the development of unbalanced contact constraints and presented with a higher rate of aneurysm rupture. Our observations are thus in agreement with the results of the International Study of Unruptured Intracranial Aneurysms (IUSUI) study showing that size and location are predictors of risk of rupture. In our opinion, this is because they predict how an aneurysm interacts with the PAE.

Several factors that have been recognized to be independent predictors of risk of rupture—such as size, location, and shape—may be assessed with current imaging investigation

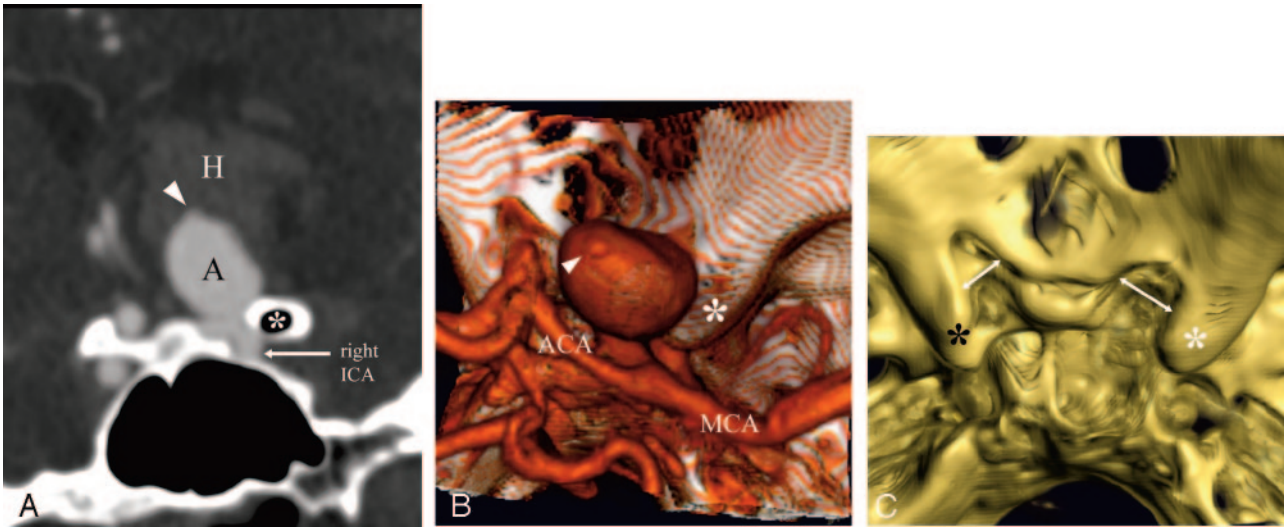

Fig 6. Ruptured, right-sided, 18-mm carotido-ophthalmic aneurysm with intraparenchymal hemorrhage into the right basal frontal lobe and basal ganglia (*A* and *B*). The aneurysm expanded superiorly and became embedded into the basal frontal lobe. It developed unbalanced contact constraints with a pneumatized, right anterior clinoid process (*A*). A contact constraint with the right optic nerve and chiasma was suspected from the location of the aneurysm, and was confirmed surgically. The aneurysm presented with a bleb at the dome (*A* and *B*). Bone 3D reconstructions revealed bony erosions of the right optic gutter and right anterior clinoid process in relation to the mass effect from the aneurysm (*C*).

A, Coronal plane, multiplanar reconstruction of the high-resolution CT angiography (HCRTA), posteroanterior view. *Asterisk,* right anterior clinoid process; *A,* aneurysm; *H,* intraparenchymal hemorrhage in the right basal ganglia; *arrowhead,* bleb.

B, 3D reconstruction of HRCTA, superior view. *Asterisk,* right anterior clinoid process; *arrowhead,* bleb.

C, 3D bone reconstruction of the base of the skull from HRCTA images. *White asterisk,* right anterior clinoid process; *black asterisk,* left anterior clinoid process; *arrows,* bony erosion of right optic gutter and right anterior clinoid process compared with the left side.

tools such as HRCTA. The present study showed that interactions between aneurysms and the PAE may be assessed by using such imaging modalities. Further efforts are necessary to confirm that the existence of an unbalanced contact constraint between an aneurysm and the PAE may represent an additional predictor of the risk of aneurysm rupture and thus help in identifying those unruptured aneurysms harboring a risk of rupture that is sufficiently high to warrant endovascular or surgical repair.

Acknowledgments

We thank Drs. Kenji Sugiu, Koji Tokunaga, Jacqueline Delavelle, and Béatrix Jean for their help in developing the concept of the PAE.

References

1. Wardlaw JM, White PM. **The detection and management of unruptured intracranial aneurysms.** *Brain* 2000;123:205–21
2. Ingall Tj, Whisnant JP, Wiebers DO, et al. **Has there been a decline in subarachnoid hemorrhage mortality?** *Stroke* 1989;20:718–24
3. ISUIA. **Unruptured intracranial aneurysms: risk of rupture and risks of surgical intervention.** *N Engl J Med* 1998;339:1725–33
4. ISUIA. **Unruptured intracranial aneurysms: natural history, clinical outcome, and risks of surgical and endovascular treatment.** *Lancet* 2003;362:103–10
5. Beck J, Rohde S, el Beltagy M, et al. **Difference in configuration of ruptured and unruptured intracranial aneurysms determined by biplanar digital subtraction angiography.** *Acta Neurochir (Wien)* 2003;145:861–65
6. Hongo K, Morota N, Watabe T, et al. **Giant basilar bifurcation aneurysm presenting as a third ventricular mass with unilateral obstructive hydrocephalus: case report.** *J Clin Neurosci* 2001;8:51–54
7. Platania N, Cutuli V, Nicoletti G, et al. **Oculomotor palsy and supraclinoid internal carotid artery aneurysms: personal experience and review of the literature.** *J Neurosurg Sci* 2002;46:107–10
8. Seshaiyer P, Humphrey JD. **On the potentially protective role of contact constraints on saccular aneurysms.** *J Biomech* 2001;34:607–12
9. Stehbens WE. **Pathology and pathogenesis of intracranial saccular aneurysms.** *Neurol Res* 1990;12:29–34
10. Suzuki J, Ohara H. **Clinicopathological study of cerebral aneurysms: origin, rupture, repair, and growth.** *J Neurosurg* 1978;48:505–14
11. Asari S, Ohmoto T. **Growth and rupture of unruptured cerebral aneurysms based on the intraoperative appearance.** *Acta Med Okayama* 1994;48:257–62
12. Tateshima S, Murayama Y, Villablanca P, et al. **In vitro measurement of fluid-induced wall shear stress in unruptured cerebral aneurysms harboring blebs.** *Stroke* 2003;34:187–92
13. Beck J, Rohde S, el Beltagy M, et al. **Difference in configuration of ruptured and unruptured intracranial aneurysms determined by biplanar digital subtraction angiography.** *Acta Neurochir* 2003;145:861–65
14. Foutrakis GN, Yonas H, Sclabassi RJ. **Saccular aneurysm formation in curved and bifurcating arteries.** *AJNR Am J Neuroradiol* 1999;29:1309–17
15. Kondo S, Hashimoto N, Kikuchi H, et al. **Cerebral aneurysms arising at non-branching sites.** *Stroke* 1997;28:398–404
16. Tateshima S, Murayama Y, Villablanca P, et al. **In vitro measurement of fluid-induced wall shear stress in unruptured cerebral aneurysms harboring blebs.** *Stroke* 2003;34:187–92
17. Mower WR, Baraff LJ, Sneyd J. **Stress distributions in vascular aneurysms: factors affecting risk of aneurysm rupture.** *J Surg Res* 1993;55:155–61
18. Chitanvis SM, Dewey M, Hademenos G, et al. **A nonlinear quasi-static model of intracranial aneurysms.** *Neurol Res* 1997;19:489–96
19. Montorzi G, Silacci P, Zulliger M, et al. **Functional, mechanical and geometrical adaptation of the arterial wall of a non-axisymmetric artery in vitro.** *J Hypertension* 2004;22:339–47